

# Optimization Algorithm Synthesis based on Integral Quadratic Constraints: A Tutorial

Carsten W. Scherer, Christian Ebenbauer and Tobias Holicki

**Abstract**—We expose in a tutorial fashion the mechanisms which underly the synthesis of optimization algorithms based on dynamic integral quadratic constraints. We reveal how these tools from robust control allow to design accelerated gradient descent algorithms with optimal guaranteed convergence rates by solving small-sized convex semi-definite programs. It is shown that this extends to the design of extremum controllers, with the goal to regulate the output of a general linear closed-loop system to the minimum of an objective function.

Numerical experiments illustrate that we can not only recover gradient decent and the triple momentum variant of Nesterov’s accelerated first order algorithm, but also automatically synthesize optimal algorithms even if the gradient information is passed through non-trivial dynamics, such as time-delays.

**Index Terms**—Optimization Algorithms, Robust Control, Linear Matrix Inequalities.

## I. INTRODUCTION

Accelerated gradient algorithms [1] have a wide range of applications in the current era of machine learning and online optimization-based control. From the perspective of control theory, such algorithms can be viewed as a linear time-invariant discrete-time (LTI) system in feedback with the gradient of the to-be-minimized function as a nonlinearity [2]–[5]. This provides an immediate link to absolute stability theory and offers the possibility to apply advanced tools from robust control for the *automated analysis* of accelerated gradient algorithms [5]. By tuning the algorithm parameters based on these tools, the convergence rate of Nesterov’s algorithm [6] has been improved to get the so-called triple momentum algorithm [7].

The *automated synthesis* of optimization algorithms by convex optimization is a much more challenging task. This falls into the area of robust feedback controller design. Recent work [8]–[10] has addressed the synthesis problem from this perspective, but based on heuristic methods without optimality guarantees. An alternative approach to non-convex algorithm design by interpolation techniques can be found in [11], [12].

The purpose of this paper is to develop, in a tutorial fashion, the whole pipeline of analysis techniques that open the avenue for a convex solution to the automated algorithm

synthesis problem by solving a moderate-sized convex semi-definite program. Another feature of the presented approach is its flexibility. It offers a convex solution to the so-called extremum control problem, with the goal to regulate the output of a dynamical system to the minimum of some convex cost function. These main results are based on [13], [14]. However, we also present an innovation over [14] which renders synthesis possible for LTI systems without any restrictions on their poles or zeros.

The paper is structured as follows. In Sec. II, we show how the algorithm analysis and synthesis problem translates into one of robustness analysis and synthesis. Sec. III recaps robustness analysis with static integral quadratic constraints (IQCs), which is extended to a version involving dynamic IQCs in Secs. IV and V. The design of algorithms is presented in Sec. VI, while numerical illustrations are found in Sec. VII. Concluding remarks are given in Sec. VIII. All proofs and some explanatory connections to classical passivity-based stability tests are found in the appendix.

Next to standard notations, for matrices  $A, B$  we express by  $A \leq B$  that  $B - A$  is nonnegative entrywise, while  $A \prec B$  means that  $A$  and  $B$  are symmetric and  $B - A$  is positive definite. For a tuple of matrices  $A = (A_1, \dots, A_k)$ , we use

$$\text{diag}(A) = \begin{pmatrix} A_1 & \cdots & 0 \\ \vdots & \ddots & \vdots \\ 0 & \cdots & A_k \end{pmatrix} \quad \text{and} \quad \text{col}(A) = \begin{pmatrix} A_1 \\ \vdots \\ A_k \end{pmatrix}$$

if the dimensions are compatible. For the real polynomial  $\alpha(z) = \alpha_0 + \cdots + \alpha_{n-1}z^{n-1} + z^n$  of degree  $n$ , we denote by  $C_\alpha \in \mathbb{R}^{n \times n}$  the standard companion matrix with the last row  $(-\alpha_0, \dots, -\alpha_{n-1})$ , and  $e_n \in \mathbb{R}^n$  is the last standard unit vector. If  $x \in \mathbb{R}^n$  then  $\|x\|^2 := x^\top x$  is the Euclidean norm. Finally,  $l_{2e}^n$  is the space of all sequences  $x : \mathbb{N}_0 \rightarrow \mathbb{R}^n$ , which are tacitly assumed to be extended as  $x_t = 0$  for  $t < 0$ .

We follow the custom in robust control to express a linear system  $x_{t+1} = Ax_t + Bu_t$ ,  $z = Cx_t + Du_t$  for  $t \in \mathbb{N}_0$  as

$$\begin{pmatrix} x_{t+1} \\ y_t \end{pmatrix} = \begin{pmatrix} A & B \\ C & D \end{pmatrix} \begin{pmatrix} x_t \\ u_t \end{pmatrix} \quad \text{or} \quad y = \left[ \begin{array}{c|c} A & B \\ \hline C & D \end{array} \right] u.$$

The latter notation is also used to represent the input-output map defined by the system. Moreover, the shorthand notation

$$\left( \begin{array}{c|c} A & B \\ \hline C & D \end{array} \right) \xrightarrow{T} \left( \begin{array}{c|c} \hat{A} & \hat{B} \\ \hline \hat{C} & \hat{D} \end{array} \right)$$

expresses that the two corresponding systems are related by a state-coordinate change with the matrix  $T$ , i.e.,  $T$  is invertible and  $\hat{A} = TAT^{-1}$ ,  $\hat{B} = TB$ ,  $\hat{C} = CT^{-1}$ ,  $\hat{D} = D$

The first and third author are funded by Deutsche Forschungsgemeinschaft (DFG, German Research Foundation) under Germany’s Excellence Strategy - EXC 2075 - 390740016. They acknowledge the support by the Stuttgart Center for Simulation Science (SimTech).

Carsten W. Scherer and Tobias Holicki are with the Department of Mathematics, University of Stuttgart, Germany (email: {carsten.scherer,tobias.holicki}@imng.uni-stuttgart.de). Christian Ebenbauer is the Chair of Intelligent Control Systems, RWTH Aachen University, Germany (email: christian.ebenbauer@ic.rwth-aachen.de).

hold true. Finally, we abbreviate Kalman's controllability matrix of the pair  $(A, B) \in \mathbb{R}^{n \times (n+m)}$  by  $\mathcal{K}(A, B) := (B, AB, \dots, A^{n-1}B)$ .

## II. OPTIMIZATION ALGORITHMS AS FEEDBACK SYSTEMS

### A. The Underlying Function Class

In this paper, we work with the class  $\mathcal{S}_{m,L}$  of functions  $f : \mathbb{R}^d \rightarrow \mathbb{R}$  that are  $L$ -smooth and  $m$ -strongly convex for  $m > 0$  or just convex if  $m = 0$ . Among the various equivalent ways to express these conditions, the following most intuitive ones do not require any a priori assumptions on differentiability.

*Definition 1:* Let  $L > m \geq 0$  and  $q(x) = \frac{1}{2}\|x\|^2$  for  $x \in \mathbb{R}^n$ . Then  $\mathcal{S}_{m,L}$  is the set of all  $f : \mathbb{R}^d \rightarrow \mathbb{R}$  such that

$$f_m := f - mq \text{ and } f^L := Lq - f \text{ are convex.}$$

Moreover, let  $\mathcal{S}_{m,L}^0 := \{f \in \mathcal{S}_{m,L} \mid f(0) = 0, \nabla f(0) = 0\}$ .

Any  $f \in \mathcal{S}_{m,L}$  is differentiable [15] and its gradient is denoted by  $\nabla f$ . It is useful to remark for  $z \in \mathbb{R}^d$  that

$$\begin{pmatrix} \nabla f^L(z) \\ \nabla f_m(z) \end{pmatrix} = \begin{pmatrix} LI & -I \\ -mI & I \end{pmatrix} \begin{pmatrix} z \\ \nabla f(z) \end{pmatrix}. \quad (1)$$

Among the many known inequalities for  $f \in \mathcal{S}_{m,L}$ , the one in the following lemma stands out in allowing for a direct construction of integral quadratic constraints. It is also underlying the proof of [5, Lemma 8] and, if evaluated at finitely many points, identical to the central inequality in [11, Theorem 4]. The proof is reproduced from [15] in Sec. X-A.

*Lemma 2:* Let  $f \in \mathcal{S}_{m,L}$ . Then the function  $V(x) := (L - m)f_m(x) - q(\nabla f_m(x))$  satisfies

$$V(u) - V(y) \leq \nabla f_m(u)^\top [\nabla f^L(u) - \nabla f^L(y)] \quad (2)$$

for all  $u, y \in \mathbb{R}^d$ . If  $f \in \mathcal{S}_{m,L}^0$  then  $V$  has a global minimum at 0 with value 0, i.e.,  $0 = V(0) \leq V(x)$  for all  $x \in \mathbb{R}^d$ .

To support the reader's intuition, we note that (2) for  $m = 0$  and  $L \rightarrow \infty$  boils down to the subgradient inequality for convex functions. Since  $f_0(x) = f(x)$ ,  $\nabla f_0(x) = \nabla f(x)$  and  $\frac{1}{L}\nabla f^L(x) \rightarrow x$  for  $L \rightarrow \infty$ , we infer  $\frac{1}{L}V(x) \rightarrow f(x)$ . After dividing (2) by  $L$ , we indeed obtain for  $m = 0$  and  $L \rightarrow \infty$  the inequality  $f(u) - f(y) \leq \nabla f(u)^\top (u - y)$ .

### B. Optimization Algorithms and Systems

For  $f \in \mathcal{S}_{m,L}$ , we recall that the optimization problem

$$\inf_{z \in \mathbb{R}^d} f(z) \quad (3)$$

does admit a unique solution  $z_*$  [16]. It is also well-known that the gradient descent algorithm

$$z_{t+1} = z_t - \alpha \nabla f(z_t) \quad (4)$$

for  $\alpha = \frac{2}{m+L}$  generates a sequence with  $\lim_{t \rightarrow \infty} z_t = z_*$ . We denote the iteration index by " $t$ " since we want to view (4) as a discrete-time dynamical system for  $t$  on the time axis  $\mathbb{N}_0$ . Even more, (4) can be viewed as the feedback interconnection of the LTI system

$$x_{t+1} = x_t - \alpha w_t, \quad z_t = x_t$$

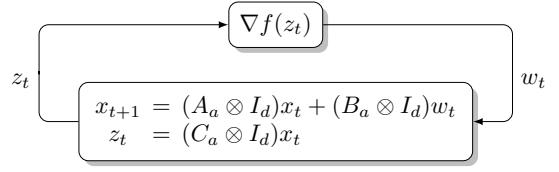


Fig. 1. Feedback representation of optimization algorithms.

with the static nonlinearity

$$w_t = \nabla f(z_t) \quad (5)$$

for  $t \in \mathbb{N}_0$ , where  $x_t \in \mathbb{R}^d$ ,  $w_t \in \mathbb{R}^d$  and  $z_t \in \mathbb{R}^d$  are the state, the input and the output of the linear system. This linear system can actually be expressed as

$$x_{t+1} = (A_a \otimes I_d)x_t + (B_a \otimes I_d)w_t, \quad z_t = (C_a \otimes I_d)x_t \quad (6)$$

where  $A_a = 1$ ,  $B_a = -\alpha$  and  $C_a = 1$ . Here  $\otimes$  denotes the Kronecker product, which is convenient to compactly describe general algorithms in the sequel. In control, the feedback interconnection (5)-(6) is a so-called Lur'e system. A block diagram of this interconnection is depicted in Fig. 1.

Accelerated versions of gradient descent include a so-called momentum term. A prominent example is Nesterov's algorithm with a description

$$v_{t+2} = v_{t+1} + \beta(v_{t+1} - v_t) - \alpha \nabla f(v_{t+1} + \gamma(v_{t+1} - v_t))$$

for suitable real parameters  $\alpha, \beta$  and  $\gamma = \beta$  [1], or the triple momentum version with  $\gamma \neq \beta$  [7]. This is nothing but

$$v_{t+2} = v_{t+1} + \beta(v_{t+1} - v_t) - \alpha w_t, \quad z_t = v_{t+1} + \gamma(v_{t+1} - v_t)$$

in feedback with (5). Moreover, the latter second order system can be routinely translated into the first-order description (6) with state  $x_t = \text{col}(v_{t+1}, v_t)$  and the matrices

$$\begin{pmatrix} A_a & B_a \\ C_a & 0 \end{pmatrix} = \begin{pmatrix} 1 + \beta & -\beta & | & -\alpha \\ 1 & 0 & | & 0 \\ 1 + \gamma & -\gamma & | & 0 \end{pmatrix}. \quad (7)$$

Hence, also Nesterov's recursion can be expressed as (5)-(6).

All this is a strong motivation for investigating the stability properties of the feedback interconnection (5)-(6) for general matrices  $(A_a, B_a, C_a)$ .

### C. Minimal Convergence Requirement

In view of the goal to solve (3), it is a minimal requirement that the interconnection (5)-(6) should have the property

$$\lim_{t \rightarrow \infty} z_t = z_* \quad \text{with} \quad \nabla f(z_*) = 0 \quad (8)$$

for any  $f \in \mathcal{S}_{m,L}$  and any initial condition.

By (5), this implies  $w_* := \lim_{t \rightarrow \infty} w_t = 0$ . If  $(A_a, C_a)$  is detectable, we infer  $\lim_{t \rightarrow \infty} x_t = x_*$  and the limit  $(x_*, w_*, z_*)$  satisfies the equilibrium equations

$$x_* = (A_a \otimes I_d)x_*, \quad z_* = (C_a \otimes I_d)x_*, \quad w_* = 0. \quad (9)$$

If we pick  $f(z) = \frac{1}{2}m\|z - z_*\|^2$  for  $z_* \in \mathbb{R}^d$  with  $z_* \neq 0$ , the corresponding solution  $x_*$  of (9) does not vanish, which in turn shows that 1 is an eigenvalue of  $A_a$ . For example in

Nesterov's algorithm, this is indeed true since the elements in each row of  $A_a$  in (7) sum up to one. As a result, the minimal requirement enforces structural constraints on the algorithm parameters  $(A_a, B_a, C_a)$ .

In general, we argue in [13, Section 2.2] that  $(A_a, C_a)$  can be assumed to be detectable without loss of generality. Then the minimal requirement implies that the algorithm parameters must admit, after a possible state-coordinate change, the structure

$$\begin{pmatrix} A_a & B_a \\ C_a & 0 \end{pmatrix} = \begin{pmatrix} A_c & B_c & 0 \\ 0 & 1 & 1 \\ C_c & D_c & 0 \end{pmatrix} \text{ with } \det \begin{pmatrix} A_c - I & B_c \\ C_c & D_c \end{pmatrix} \neq 0. \quad (10)$$

The first relation means that the system described with  $(A_a, B_a, C_a)$  is the series interconnection of

$$\begin{pmatrix} x_{t+1}^c \\ z_t \end{pmatrix} = \begin{pmatrix} A_c \otimes I_d & B_c \otimes I_d \\ C_c \otimes I_d & D_c \otimes I_d \end{pmatrix} \begin{pmatrix} x_t^c \\ y_t \end{pmatrix} \quad (11)$$

and the discrete-time integrator

$$\begin{pmatrix} x_{t+1}^s \\ y_t \end{pmatrix} = \begin{pmatrix} I_d & I_d \\ I_d & 0 \end{pmatrix} \begin{pmatrix} x_t^s \\ w_t \end{pmatrix} \quad (12)$$

with the transfer matrix  $\frac{1}{z-1}I_d$ . The second condition in (10) expresses the fact that the pole  $z = 1$  of the integrator in the corresponding product of transfer matrices is not canceled.

In other words, the algorithm parameters must contain a model of the integrator. Although not surprising from the perspective of control, this fact has only been recently clearly emphasized in [9], [13] in the realm of algorithm analysis.

As an illustration, for (7) we note that

$$\begin{pmatrix} 1+\beta & -\beta & -\alpha \\ 1 & 0 & 0 \\ 1+\gamma & -\gamma & 0 \end{pmatrix} \begin{pmatrix} 0 & \frac{1}{\alpha} \\ -\frac{1}{\alpha} & \frac{\beta}{\alpha} \end{pmatrix} \begin{pmatrix} \beta & -\alpha & 0 \\ 0 & 1 & 1 \\ \beta(1+\gamma)-\gamma & -\alpha(1+\gamma) & 0 \end{pmatrix}.$$

Let us now pinpoint the two essential consequences in case that  $(A_a, B_a, C_a)$  does indeed have the structure (10):

- 1) If (8) is satisfied for (5)-(6) and all  $f \in \mathcal{S}_{m,L}^0$ , then (8) holds for (5)-(6) and all  $f \in \mathcal{S}_{m,L}$ .
- 2) The interconnection (5)-(6) is a controlled uncertain system as familiar in robust control.

To see 1), we assign to any  $f \in \mathcal{S}_{m,L}$  the function  $f_*$ , defined with the unique  $z_* \in \mathbb{R}^d$  satisfying  $\nabla f(z_*) = 0$  as

$$f_*(z) := f(z + z_*) - f(z_*) \text{ for } z \in \mathbb{R}^d.$$

Since  $f_*(0) = 0$  and  $\nabla f_*(0) = 0$ , we note that  $f_* \in \mathcal{S}_{m,L}^0$ . If  $x_*$  denotes the unique solution of (9), the system (6) can be equivalently transformed into

$$\begin{aligned} x_{t+1} - x_* &= (A_a \otimes I_d)(x_t - x_*) + (B_a \otimes I_d)w_t, \\ z_t - z_* &= (C_a \otimes I_d)(x_t - x_*). \end{aligned}$$

To be precise, the trajectories  $(x, w, z)$  of the interconnection (5)-(6) are in one-to-one correspondence via  $\tilde{x} = x - x_*$ ,  $\tilde{w} = w$ ,  $\tilde{z} = z - z_*$  with the trajectories  $(\tilde{x}, \tilde{w}, \tilde{z})$  of (6) in feedback with

$$\tilde{w}_t = \nabla f_*(\tilde{z}_t). \quad (13)$$

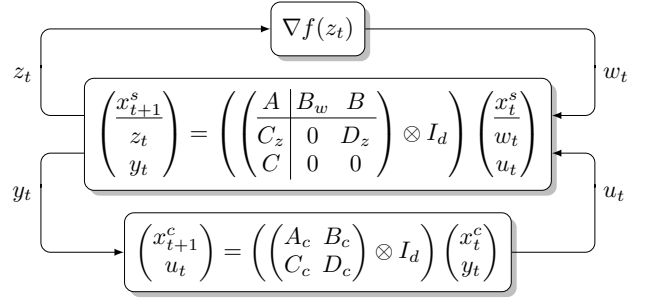


Fig. 2. General algorithm synthesis configuration.

This proves 1). Even stronger, it shows that any stability property of (6), (13) with respect to the equilibrium  $(\tilde{x}_*, \tilde{w}_*, \tilde{z}_*) = (0, 0, 0)$  is equivalent to the same stability property of (5)-(6) with respect to the equilibrium  $(x_*, 0, z_*)$ .

Property 2) is seen by redrawing Fig. 1 as in Fig. 2 with

$$\begin{pmatrix} A & B_w & B \\ C_z & 0 & D_z \\ C & 0 & 0 \end{pmatrix} = \begin{pmatrix} 1 & 1 & 0 \\ 0 & 0 & 1 \\ 1 & 0 & 0 \end{pmatrix}, \quad (14)$$

by recalling (11)-(12) and using the auxiliary signal  $u_t := z_t$ . Then we indeed recognize the uncertainty  $\nabla f$  in the class  $\nabla \mathcal{S}_{m,L}^0$ , the to-be-controlled plant defined with (14) and the controller (11). We also emphasize the simplicity of this plant in the realm of algorithms! Still, it is relevant to stress that all our subsequent analysis and synthesis results even apply to general LTI plants as in Fig. 2.

### III. EXPONENTIAL STABILITY AND PASSIVITY

Let us now turn to the development of a test which ensures that the loop (5)-(6) is exponentially stable for all  $f \in \mathcal{S}_{m,L}^0$ .

One way is based on the exponential signal weighting map

$$T_{\rho^{-1}}(z_0, z_1, z_2, \dots) = (z_0, \rho^{-1}z_1, \rho^{-2}z_2, \dots) \quad (15)$$

for some  $\rho \in (0, 1)$  [17]. Clearly,  $T_{\rho^{-1}}$  is linear and invertible with  $T_{\rho^{-1}}^{-1} = T_{\rho}$ . It is then easily checked that the set of trajectories  $(x, w, z)$  of (6) are in one-to-one correspondence with trajectories  $(\bar{x}, \bar{w}, \bar{z})$  of the system

$$\begin{aligned} \bar{x}_{t+1} &= (\bar{A}_a \otimes I_d)\bar{x}_t + (\bar{B}_a \otimes I_d)\bar{w}_t, \\ \bar{z}_t &= (C_a \otimes I_d)\bar{x}_t \end{aligned} \quad (16)$$

under the signal transformations  $\bar{x} = T_{\rho^{-1}}x$ ,  $\bar{w} = T_{\rho^{-1}}w$ , and  $\bar{z} = T_{\rho^{-1}}z$  and with the scaled matrices

$$(\bar{A}_a \ \bar{B}_a) := \rho^{-1} (A \ B).$$

Similarly, (5) translates into

$$\bar{w}_t = \bar{F}(t, \bar{z}_t) \quad (17)$$

with the static time-varying map  $\bar{F}$  associated to  $\nabla f$  through

$$\bar{F}(t, z) := \rho^{-t} \nabla f(\rho^t z) \text{ for } t \in \mathbb{N}_0, z \in \mathbb{R}^d. \quad (18)$$

The bars should remind us that  $(\bar{A}, \bar{B})$  and  $\bar{F}$  depend on  $\rho$ .

As a consequence, if the transformed loop is Lyapunov stable in the sense of  $\|\bar{x}_t\| \leq K\|\bar{x}_0\|$  for all  $t \in \mathbb{N}_0$ , one can conclude that the original loop is exponentially stable with

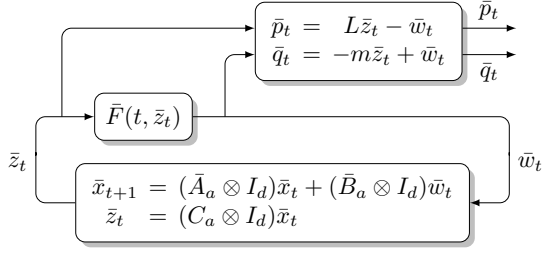


Fig. 3. Block diagram of transformed loop (16)-(17) with signals filtered according to (22).

rate  $\rho$  in the sense of  $\|x_t\| \leq K\rho^{-t}\|x_0\|$  for all  $t \in \mathbb{N}_0$ . This motivates to develop a robust stability test for the transformed interconnection (16)-(17).

We start by deriving what is called a valid integral quadratic constraint (IQC) for the nonlinearity by exploiting Lemma 2. If  $f \in \mathcal{S}_{m,L}^0$ , we conclude from (2) for  $y = 0$  that

$$V(u) \leq \nabla f_m(u)^\top \nabla f^L(u) \quad \text{for all } u \in \mathbb{R}^d. \quad (19)$$

Since  $V$  is nonnegative and  $\rho > 0$ , this trivially implies

$$0 \leq \rho^{-t} \nabla f_m(\rho^t z_t)^\top (\rho^{-t} \nabla f^L(\rho^t z_t))$$

for all  $z \in l_{2e}^d$  and  $t \in \mathbb{N}_0$ . Summation leads to the IQC

$$0 \leq \sum_{t=0}^{T-1} \bar{F}_m(t, \bar{z}_t)^\top \bar{F}^L(t, \bar{z}_t) \quad \text{for all } T \in \mathbb{N} \quad (20)$$

and all sequences  $\bar{z} \in l_{2e}^d$ . In here,  $\bar{F}_m$  and  $\bar{F}^L$  are as well defined according to (18). Note that the misnomer results from a similar concept for continuous-time systems, in which summation is replaced by integration [18]. With (1) we infer

$$\begin{pmatrix} \bar{F}^L(t, \bar{z}_t) \\ \bar{F}_m(t, \bar{z}_t) \end{pmatrix} = \begin{pmatrix} LI_d & -I_d \\ -mI_d & I_d \end{pmatrix} \begin{pmatrix} \bar{z}_t \\ \bar{F}(t, \bar{z}_t) \end{pmatrix}. \quad (21)$$

This motivates to introduce the static filter

$$\begin{pmatrix} \bar{p}_t \\ \bar{q}_t \end{pmatrix} = \begin{pmatrix} LI_d & -I_d \\ -mI_d & I_d \end{pmatrix} \begin{pmatrix} \bar{z}_t \\ \bar{w}_t \end{pmatrix}. \quad (22)$$

If filtering the input-output signals of the nonlinearity (17) accordingly, (21) shows  $\bar{p}_t = \bar{F}^L(t, \bar{z}_t)$  and  $\bar{q}_t = \bar{F}_m(t, \bar{z}_t)$ . Then (20) reads as  $\sum_{t=0}^{T-1} \bar{q}_t^\top \bar{p}_t \geq 0$  for all  $T \in \mathbb{N}$  and can be interpreted as a passivity property [17] for the outputs of (22) driven by the signals in (17).

In view of Fig. 3 and motivated by the passivity theorem, we expect that stability of (16)-(17) is guaranteed in case that  $\sum_{t=0}^{T-1} \bar{q}_t^\top \bar{p}_t < 0$  holds for all  $T \in \mathbb{N}$  along the input-output trajectories of the linear system (16) filtered with (22).

To make this precise, we start by emphasizing that the stability test itself is formulated for  $d = 1$ , while the conclusions are drawn for arbitrary dimensions  $d \in \mathbb{N}$ . All throughout the paper we slightly abuse the notation and do not indicate the dependence of system signals on  $d$ .

For  $d = 1$ , we note that the input-output signals of (16) filtered with (22) satisfy  $\bar{w}_t = mC_a \bar{x}_t + \bar{q}_t$  and  $\bar{p}_t = LC_a \bar{x}_t -$

$\bar{w}_t$ . With an identical state-trajectory, we hence infer

$$\begin{pmatrix} \bar{x}_{t+1} \\ \bar{p}_t \end{pmatrix} = \underbrace{\begin{pmatrix} \bar{A}_a + \bar{B}_a m C_a & \bar{B}_a \\ (L - m) C_a & -1 \end{pmatrix}}_{\begin{pmatrix} \mathcal{A} & \mathcal{B} \\ \mathcal{C} & \mathcal{D} \end{pmatrix}} \begin{pmatrix} \bar{x}_t \\ \bar{q}_t \end{pmatrix}. \quad (23)$$

As a consequence, also for a general  $d \in \mathbb{N}$ , the trajectories of (16) filtered with (22) satisfy

$$\begin{pmatrix} \bar{x}_{t+1} \\ \bar{p}_t \end{pmatrix} = \begin{pmatrix} \mathcal{A} \otimes I_d & \mathcal{B} \otimes I_d \\ \mathcal{C} \otimes I_d & \mathcal{D} \otimes I_d \end{pmatrix} \begin{pmatrix} \bar{x}_t \\ \bar{q}_t \end{pmatrix}. \quad (24)$$

All this leads to our first analysis result, which involves a passivity property of the system (23) and hence also of (24).

**Theorem 3:** Suppose there exists some  $\mathcal{X} = \mathcal{X}^\top$  with

$$\mathcal{X} \succ 0 \text{ and } \begin{pmatrix} \mathcal{A} & \mathcal{B} \\ I & 0 \end{pmatrix}^\top \begin{pmatrix} \mathcal{X} & 0 \\ 0 & -\mathcal{X} \end{pmatrix} \begin{pmatrix} \mathcal{A} & \mathcal{B} \\ I & 0 \end{pmatrix} + \begin{pmatrix} \mathcal{C} & \mathcal{D} \\ 0 & 1 \end{pmatrix}^\top \begin{pmatrix} 0 & 1 \\ 1 & 0 \end{pmatrix} \begin{pmatrix} \mathcal{C} & \mathcal{D} \\ 0 & 1 \end{pmatrix} \prec 0. \quad (25)$$

Then there exists a constant  $K$  such that, for any  $f \in \mathcal{S}_{m,L}^0$ , all trajectories of the original loop (5)-(6) satisfy

$$\|x_t\| \leq K\rho^t \|x_0\| \quad \text{for all } t \in \mathbb{N}_0. \quad (26)$$

For  $\rho = 1$ , it is also assured that  $\lim_{t \rightarrow \infty} x_t = 0$  holds true.

The dissipativity-based proof is found in Sec. X-B.

Before addressing the practical application of this robust stability test, we discuss how to reduce the conservatism by the incorporation of so-called stability multipliers.

#### IV. DYNAMIC INTEGRAL QUADRATIC CONSTRAINTS

It is a classical idea [19], [20] to improve Theorem 3 by imposing a passivity condition after filtering the signal  $\bar{p}$  in (22) with a causal and stable time-invariant system. In this context, such a filter is often called a stability multiplier [17].

In fact, passing the signal  $\bar{p}_t = \bar{F}^L(t, \bar{z}_t)$  through a delay of time  $\nu \in \mathbb{N}$  leads to  $\bar{r}_t = \bar{F}^L(t - \nu, \bar{z}_{t-\nu})$  (where we recall our convention that  $\bar{z}_{t-\nu} = 0$  and hence  $\bar{r}_{t-\nu} = 0$  for  $t < \nu$ .) The following IQC incorporates this delayed signal  $\bar{r}_t$  and is, again, a rather immediate consequence of Lemma 2. The proof is found in Sec. X-C.

**Lemma 4:** Let  $f \in \mathcal{S}_{m,L}^0$ ,  $\rho \in (0, 1]$  and  $\nu \in \mathbb{N}$ . Then

$$0 \leq \sum_{t=0}^{T-1} \bar{F}_m(t, \bar{z}_t)^\top (\bar{F}^L(t, \bar{z}_t) - \rho^\nu \bar{F}^L(t - \nu, \bar{z}_{t-\nu})) \quad (27)$$

holds for all  $T \in \mathbb{N}$  and all signals  $\bar{z} \in l_{2e}^d$ .

A conic combination of (20) and (27) for  $\nu \in \mathbb{N}$  leads to the IQC with more general filters in the following lemma. The proof is given in Sec. X-D.

**Lemma 5:** Let  $f \in \mathcal{S}_{m,L}^0$ ,  $\rho \in (0, 1]$  and suppose that  $\lambda_0, \lambda_1, \dots \in \mathbb{R}$  satisfy

$$\lambda_\nu \leq 0 \quad \text{for all } \nu \in \mathbb{N} \quad \text{and} \quad \sum_{\nu=0}^{\infty} \rho^{-\nu} \lambda_\nu > 0. \quad (28)$$

For  $\bar{z} \in l_{2e}^d$ , let  $\bar{p}_t = \bar{F}^L(t, \bar{z}_t)$  be passed through the filter

$$\bar{r}_t = \sum_{\nu=0}^t \lambda_\nu \bar{p}_{t-\nu} \quad \text{for } t \in \mathbb{N}_0. \quad (29)$$

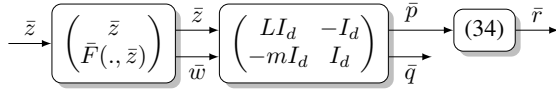


Fig. 4. Signals in dynamic IQC of nonlinearity.

With  $\bar{q}_t := \bar{F}_m(t, \bar{z}_t)$ , the signals  $\bar{r}, \bar{q}$  then satisfy the IQC

$$0 \leq \sum_{t=0}^{T-1} \bar{q}_t^\top \bar{r}_t \text{ for all } T \in \mathbb{N}. \quad (30)$$

Due to the incorporation of the dynamic filter (29), we call (30) a dynamic IQC. Note that (28) implies  $\lambda_0 > 0$ . Replacing the last constraint in (28) by  $\sum_{\nu=0}^{\infty} \rho^{-\nu} \lambda_\nu \geq 0$  just includes the trivial case  $\lambda_\nu = 0$  for all  $\nu \in \mathbb{N}_0$ , which justifies our choice to work with the strict inequality only.

The infinite impulse response filters (29) are subject to the infinite number of constraints (28). To overcome this trouble, we proceed with filters that have a state-space realization  $(A_f, B_f, C_f, D_f)$  with a fixed pole-pair  $(A_f, B_f) \in \mathbb{R}^{l \times (l+1)}$  and free filter coefficients collected in  $(C_f, D_f) \in \mathbb{R}^{1 \times (l+1)}$  such that

$$\lambda_0 = D_f \text{ and } \lambda_{\nu+1} = C_f A_f^\nu B_f \text{ for } \nu \in \mathbb{N}_0. \quad (31)$$

The boldface notation reminds us of the fact that  $(C_f, D_f)$  is a decision variable in the subsequent stability test. For a suitable choice of  $(A_f, B_f)$ , we now establish that the infinitely many constraints (28) on the Markov parameters (31) can be expressed by a finite number of linear ones.

**Lemma 6:** Fix  $(A_f, B_f) = (C_\alpha, e_l)$  with a real polynomial  $\alpha(z) = \alpha_0 + \alpha_1 z + \dots + \alpha_{l-1} z^{l-1} + z^l$  of degree  $l \in \mathbb{N}$  having all its roots in  $\mathbb{D}_\rho := \{z \in \mathbb{C} \mid |z| < \rho\}$  and coefficients satisfying  $\alpha_0, \dots, \alpha_{l-1} \leq 0$ .

Then, for any pair  $(C_f, D_f) \in \mathbb{R}^{1 \times (l+1)}$ , the Markov parameters (31) satisfy the constraints (28) iff

$$C_f \mathcal{K}(A_f, B_f) \leq 0 \text{ and } D_f + C_f(\rho I - A_f)^{-1} B_f > 0. \quad (32)$$

Moreover, (32) implies that  $D_f > 0$  and that all eigenvalues of  $A_f - B_f D_f^{-1} C_f$  are located in  $\mathbb{D}_\rho$ .

The proof is given in Sec. X-E.

To summarize, for a fixed polynomial  $\alpha$  of degree  $l$  as in Lemma 6, we work from now on with the filter matrices

$$A_f := C_\alpha, \quad B_f := e_l, \quad C_f \in \mathbb{R}^{1 \times l}, \quad D_f \in \mathbb{R} \quad (33)$$

such that  $(C_f, D_f)$  satisfies the constraints (32). It is then assured that the trajectories of (17) filtered by (22) and

$$\begin{pmatrix} \xi_{t+1} \\ \bar{r}_t \end{pmatrix} = \begin{pmatrix} A_f \otimes I_d & B_f \otimes I_d \\ C_f \otimes I_d & D_f \otimes I_d \end{pmatrix} \begin{pmatrix} \xi_t \\ \bar{p}_t \end{pmatrix}, \quad \xi_0 = 0 \quad (34)$$

as depicted in Fig. 4 satisfy the passivity condition (30) for all  $f \in \mathcal{S}_{m,L}^0$ . In this way, we have identified a whole nicely parameterized convex family of valid dynamic IQCs involving the filter or multiplier (34) for the nonlinearity (17).

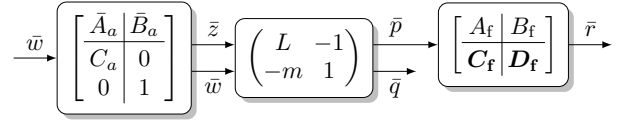


Fig. 5. Signals in filtered linear system.

## V. ROBUST STABILITY ANALYSIS WITH DYNAMIC IQCS

In alignment with Sec. III, the robust stability test is formulated for the correspondingly filtered linear system as depicted in Fig. 5. If recalling (23), we are lead to the system

$$\bar{r} = \begin{bmatrix} A_f & B_f \\ C_f & D_f \end{bmatrix} \begin{bmatrix} \bar{A}_a + \bar{B}_a m C_a & \bar{B}_a \\ (L - m) C_a & -1 \end{bmatrix} \bar{q}.$$

A realization of this series interconnection is given as

$$\begin{pmatrix} \mathcal{A} & \mathcal{B} \\ \mathcal{C} & \mathcal{D} \end{pmatrix} := \begin{pmatrix} A_f & B_f(L - m)C_a & -B_f \\ 0 & \rho^{-1}(A_a + B_a m C_a) & \rho^{-1}B_a \\ C_f & D_f(L - m)C_a & -D_f \end{pmatrix}. \quad (35)$$

Here and in the sequel, the boldface notation for the new matrices indicates that they depend affinely on the decision variables  $(C_f, D_f)$ .

**Theorem 7:** Suppose there exists some  $\mathcal{X} = \mathcal{X}^\top$  and a filter parameter vector  $(C_f, D_f)$  with (32) such that (25) is satisfied if replacing  $(\mathcal{A}, \mathcal{B}, \mathcal{C}, \mathcal{D})$  by  $(\mathcal{A}, \mathcal{B}, \mathcal{C}, \mathcal{D})$  in (35). Then the same conclusions can be drawn as in Theorem 3.

The proof is an extension of the one for Theorem 3 and given in Section X-F.

After picking a characteristic filter polynomial  $\alpha$  of degree  $l$  and the targeted convergence rate  $\rho \in (0, 1]$ , feasibility of (25) with (35) thus guarantees exponential stability of (5)-(6) with rate  $\rho$  for all trajectories and any  $f \in \mathcal{S}_{m,L}^0$  for arbitrary dimensions  $d \in \mathbb{N}$ . Since  $(\mathcal{C}, \mathcal{D})$  is affine in  $(C_f, D_f)$ , this involves testing the feasibility of a genuine LMI in the variables  $(C_f, D_f)$  and  $\mathcal{X}$  whose dimension is independent from  $d \in \mathbb{N}$ . A more detailed practical recipe for how to apply Theorem 7 can be extracted from Sec. VI.

Let us emphasize that Theorem 7 encompasses Theorem 3 if  $(A_f, B_f, C_f)$  are empty ( $l = 0$ ); then the LMI (25) is homogeneous in  $(\mathcal{X}, \mathcal{D})$ , which permits to fix  $\mathcal{D} = D_f$  to 1 without loss of generality. It is remarkable that even a few filter states often substantially improve the test over  $l = 0$ .

Also note that Theorem 7 for  $\alpha(z) = z^l$  with  $l = 1$  encompasses the algorithm analysis approach in [5]. Related IQC results to ensure robust exponential loop stability can be found in [21], [22].

Some explanatory connections of Theorems 3 and 7 with classical passivity-based stability tests are discussed in Sec. IX. We finally stress that the developed IQCs can be embedded into a much more general dissipativity-based robustness analysis framework as exposed in the recent survey article [23] and the references therein.

## VI. CONVEX ALGORITHM SYNTHESIS

Let us now turn to the design problem for the interconnection in Fig. 2 with the general plant

$$\begin{pmatrix} z \\ y \end{pmatrix} = \left[ \begin{array}{c|cc} A & B_w & B \\ \hline C_z & 0 & D_z \\ \hline C & 0 & 0 \end{array} \right] \begin{pmatrix} w \\ u \end{pmatrix} \quad (36)$$

where  $A \in \mathbb{R}^{n \times n}$ . Again, we slightly abuse notation by not indicating the dependence of the signals on  $d$ . As for analysis, we first construct the modified system description in order to formulate the key synthesis result. To this end, we transform all signals of (36) according to (15) to get

$$\begin{pmatrix} \bar{z} \\ \bar{y} \end{pmatrix} = \left[ \begin{array}{c|cc} \rho^{-1}A & \rho^{-1}B_w & \rho^{-1}B \\ \hline C_z & 0 & D_z \\ \hline C & 0 & 0 \end{array} \right] \begin{pmatrix} \bar{w} \\ \bar{u} \end{pmatrix}.$$

Filtering the signal  $\text{col}(\bar{z}, \bar{w})$  as in (22) with  $d = 1$  leads to

$$\bar{p} = \underbrace{\left[ \begin{array}{c|cc} \rho^{-1}(A+B_w m C_z) & \rho^{-1}B_w & \rho^{-1}(B+B_w m D_z) \\ \hline (L-m)C_z & -1 & (L-m)D_z \end{array} \right]}_{\left[ \begin{array}{c|cc} \tilde{A} & \tilde{B}_w & \tilde{B} \\ \hline \tilde{C}_z & \tilde{D}_{zw} & \tilde{D}_z \end{array} \right]} \begin{pmatrix} \bar{q} \\ \bar{u} \end{pmatrix}.$$

The  $\rho$ -weighted plant filtered with (34) for  $d = 1$  reads as

$$\begin{pmatrix} \bar{r} \\ \bar{y} \end{pmatrix} = \underbrace{\left[ \begin{array}{cc|cc} A_f & B_f \tilde{C}_z & B_f \tilde{D}_{zw} & B_f \tilde{D}_z \\ 0 & \tilde{A} & \tilde{B}_w & \tilde{B} \\ \hline C_f & D_f \tilde{C}_z & D_f \tilde{D}_{zw} & D_f \tilde{D}_z \\ 0 & C & 0 & 0 \end{array} \right]}_{\left[ \begin{array}{c|cc} \tilde{A} & \tilde{B}_w & \tilde{B} \\ \hline \tilde{C}_z & \tilde{D}_{zw} & \tilde{D}_z \\ \hline \tilde{C} & 0 & 0 \end{array} \right]} \begin{pmatrix} \bar{q} \\ \bar{u} \end{pmatrix}. \quad (37)$$

For the system (37), we now pick a controller

$$\bar{u} = \left[ \begin{array}{c|c} \hat{A}_c & \hat{B}_c \\ \hline \hat{C}_c & \hat{D}_c \end{array} \right] \bar{y}. \quad (38)$$

Then the resulting interconnection admits the description

$$\bar{r} = \left[ \begin{array}{c|cc} \hat{A} + \hat{B} \hat{D}_c \hat{C} & \hat{B} \hat{C}_c & \hat{B}_w \\ \hline \hat{B}_c \hat{C} & \hat{A}_c & 0 \\ \hline \hat{C}_z + \hat{D}_z \hat{D}_c \hat{C} & \hat{D}_z \hat{C}_c & \hat{D}_{zw} \end{array} \right] \bar{q} =: \left[ \begin{array}{c|c} \mathcal{A} & \mathcal{B} \\ \hline \mathcal{C} & \mathcal{D} \end{array} \right] \bar{q}, \quad (39)$$

where all the bold matrices depend affinely on  $(C_f, D_f)$ .

If (38) is a controller for which the controlled system (39) satisfies the hypotheses of Theorem 7, it is not difficult to verify that the original plant (36) controlled with

$$u = \left[ \begin{array}{c|c} \rho \hat{A}_c & \rho \hat{B}_c \\ \hline \hat{C}_c & \hat{D}_c \end{array} \right] y$$

and resulting in the interconnection of Figure 2 satisfies (26) for any initial condition and any  $f \in \mathcal{S}_{m,L}^0$ .

Let us now recap a solution for the design problem if  $(C_f, D_f)$  satisfying (32) is *held fixed*. To this end, we pick so-called annihilator matrices  $\hat{U}$  and  $\hat{V}$  with

$$\hat{U} = \text{diag}(\hat{C}_\perp, 1) \quad \text{and} \quad \hat{V}^\top = (\hat{B}^\top \quad \hat{E}^\top)_\perp \quad (40)$$

where  $M_\perp$  means that the columns of this matrix form a basis of the kernel of the matrix  $M$ . Then there exist a controller (38) for (37) such that the closed loop system (39) renders the analysis LMIs in Theorem 7 feasible iff there exist symmetric matrices  $X$  and  $\hat{Y}$  which satisfy

$$\bullet^\top \left( \begin{array}{cc|cc} X & 0 & 0 & 0 \\ 0 & -X & 0 & 0 \\ \hline 0 & 0 & 0 & 1 \\ 0 & 0 & 1 & 0 \end{array} \right) \left( \begin{array}{c|c} \hat{A} & \hat{B}_1 \\ \hline I & 0 \\ \hline \tilde{C}_z & \tilde{D}_{zw} \\ 0 & 1 \end{array} \right) \hat{U} \prec 0, \quad (41)$$

$$\hat{V} \left( \begin{array}{cc|cc} -I & \hat{A} & 0 & \hat{B}_1 \\ 0 & \tilde{C}_z & -1 & \tilde{D}_{zw} \end{array} \right) \left( \begin{array}{c|cc} \hat{Y} & 0 & 0 & 0 \\ 0 & -\hat{Y} & 0 & 0 \\ \hline 0 & 0 & 0 & 1 \\ 0 & 0 & 1 & 0 \end{array} \right) \bullet^\top \succ 0, \quad (42)$$

$$\left( \begin{array}{c|c} \hat{Y} & I \\ \hline I & X \end{array} \right) \succ 0. \quad (43)$$

This is a slight variant of a seminal result obtained by [24], [25]. For fixed  $(C_f, D_f)$ , these constraints are affine in  $X$  and  $\hat{Y}$ . However, this nice structural property is destroyed for (42) if viewing  $(C_f, D_f)$  as an additional decision variable.

To overcome this trouble, we note that the subsystem  $\bar{u} \rightarrow \bar{r}$  of (37) is actually given by

$$\bar{r} = \left[ \begin{array}{c|c} A_f & B_f \\ \hline C_f & D_f \end{array} \right] \left[ \begin{array}{c|c} \tilde{A} & \tilde{B} \\ \hline \tilde{C}_z & \tilde{D}_z \end{array} \right] \bar{u} = \left[ \begin{array}{c|c} \tilde{A} & \tilde{B} \\ \hline \tilde{C}_z & \tilde{D}_z \end{array} \right] \left[ \begin{array}{c|c} A_f & B_f \\ \hline C_f & D_f \end{array} \right] \bar{u}, \quad (44)$$

which is a series interconnection of two commuting SISO systems. As the key to convexification, this commutation is reflected in a corresponding state-coordinate change for the corresponding natural realizations as

$$\left[ \begin{array}{cc|c} A_f & B_f \tilde{C}_z & B_f \tilde{D}_z \\ 0 & \tilde{A} & \tilde{B} \\ \hline C_f & D_f \tilde{C}_z & D_f \tilde{D}_z \end{array} \right] \xrightarrow{T} \left[ \begin{array}{cc|c} A_f & 0 & B_f \\ \tilde{B} C_f & \tilde{A} & \tilde{B} D_f \\ \hline \tilde{D}_z C_f & \tilde{C}_z & \tilde{D}_z D_f \end{array} \right]$$

with the specifically structured transformation matrix

$$T = \begin{pmatrix} L^{-1} & -L^{-1}K \\ NL^{-1} & M - NL^{-1}K \end{pmatrix} = \begin{pmatrix} T_f \\ \tilde{T} \end{pmatrix}. \quad (45)$$

The precise result is formulated in Lemma 9 in Section X-H. An analogous commutation property is used for convexification in [13] based on the Youla-Parametrization and in the state-space approach of [14]. The latter is confined to  $\alpha(z) = z^l$  for the characteristic polynomial of  $A_f$ , which induces some limitation on the plant (37). None are required in the next result due to the novel flexibility of choosing  $\alpha$ .

**Theorem 8:** Pick  $\alpha$  as in Lemma 6 such that the eigenvalues of  $A_f$  are different from the eigenvalues of  $\tilde{A}$  and from the zeros of  $\tilde{C}_z(zI - \tilde{A})^{-1}\tilde{B} + \tilde{D}_z$ . With the solutions  $K, L, M$  and  $N$  of the linear equations

- 1)  $A_f K - K \tilde{A} + B_f \tilde{C}_z = 0$ ,
- 2)  $L K(A_f, B_f) = K(A_f, B_f \tilde{D}_z - K \tilde{B})$ ,
- 3)  $M \alpha(\tilde{A}) = D_f \alpha(\tilde{A}) + (C_f \otimes I_l) \text{col}(I, \tilde{A}, \dots, \tilde{A}^{l-1})$ ,
- 4)  $\tilde{A} N - N A_f + B C_f = 0$ ,

define  $\tilde{T} = (NL^{-1} \quad M - NL^{-1}K)$ . Moreover, let

$$\hat{U} = \text{diag}(I, \tilde{C}_\perp, 1) \quad \text{and} \quad V^\top = (\tilde{B}^\top \quad \tilde{D}_z^\top)_\perp. \quad (46)$$

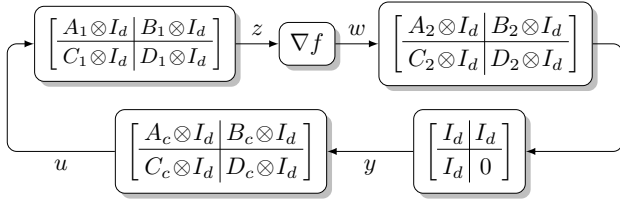


Fig. 6. Optimization over communication channels.

Then the following statements are equivalent.

- (a) There exists a controller (38) for the plant (37) such that the controlled interconnection (39) satisfies the hypotheses in Theorem 7.
- (b) There exist  $(C_f, D_f)$  satisfying (32) and symmetric matrices  $X, \tilde{Y}$  satisfying the LMIs (41) together with

$$V \begin{pmatrix} -I & \tilde{A} & 0 \\ 0 & \tilde{C}_z & -1 \end{pmatrix} \begin{pmatrix} \tilde{T} \tilde{B}_1 \\ \tilde{D}_{zw} \end{pmatrix} \begin{pmatrix} \tilde{Y} & 0 & 0 \\ 0 & -\tilde{Y} & 0 \\ 0 & 0 & 0 \\ 0 & 0 & 1 \end{pmatrix} \bullet^\top \succ 0, \quad (47)$$

$$\begin{pmatrix} \tilde{Y} & \tilde{T} \\ \tilde{T}^\top & X \end{pmatrix} \succ 0. \quad (48)$$

Note that  $\tilde{T}$  depends *affinely* on  $(C_f, D_f)$  and, thus, the constraints (32), (41) and (47)-(48) constitute *affine constraints on all decision variable*  $(C_f, D_f)$ ,  $X$  and  $\tilde{Y}$ . Hence, their feasibility can be verified by standard SDP-solvers. Once  $(C_f, D_f)$  has been determined, a standard construction leads to a suitable controller for which the hypothesis of Theorem 7 are satisfied. A numerically stable and constructive procedure based on the classical synthesis conditions (41)-(43) is found, e.g., in [26]. The dimension of the resulting state-matrix  $A_c$  equals that of  $A$ .

For a particular choice of  $(A_f, B_f)$ , let us now summarize a concrete recipe for how to synthesize controllers:

- 1) Choose  $0 < m < L$ ,  $\rho \in (0, 1]$  and  $z_0 \in [0, \rho)$ .
- 2) Pick  $l \in \mathbb{N}$  and  $A_f = C_\alpha$ ,  $B_f = e_l$  for  $\alpha(z) = z^l - z_0$ . For  $l = 0$ , take  $(A_f, B_f, C_f)$  to be empty and  $D_f := 1$ .
- 3) With (37), set up the system of LMIs (32), (41) and (47)-(48) in the variables  $(C_f, D_f)$ ,  $X$  and  $\tilde{Y}$ .

If the resulting LMIs are feasible, one can construct a controller such that all trajectories of the interconnection in Fig. 2 decay exponentially with rate  $\rho$ . A bisection strategy permits to determine the best possible (infimal) rate  $\rho_*$  depending on  $m, L, l$  and  $z_0$ . If  $\rho > \rho_*$  is very close to the optimal value  $\rho_*$ , it is typical that the left-hand side in the coupling condition (43) has an almost vanishing eigenvalue, which permits to reduce the size of the controller.

Let us finally emphasize that the synthesis LMIs are not depending on  $d$ , and that their complexity is determined by the dimensions of  $A$  and  $A_f$  only.

## VII. NUMERICAL ILLUSTRATIONS

We illustrate our results by an extremum control problem. The purpose is to design an algorithm which minimizes any  $f \in \mathcal{S}_{m,L}$ . During the iteration, the algorithm needs to transmit the actual iterate  $u_t$  via a communication channel

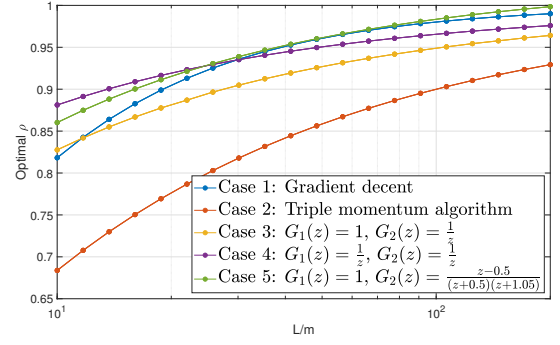


Fig. 7. Optimal convergence rates plotted over  $\frac{L}{m}$  for  $z_0 = 10^{-4}$  and  $l = 2$  and for various communication dynamics.

modeled by some LTI system  $(A_1, B_1, C_1, D_1)$  with transfer function  $G_1(z)$  to generate  $z_t$ . This is fed into the gradient to return  $w_t = \nabla f(z_t)$ . In turn, this signal is communicated back to the algorithm via a channel  $(A_2, B_2, C_2, D_2)$  with transfer function  $G_2(z)$ . To enforce integral action in the loop, we are led to the configuration in Fig. 6 with to-be-designed algorithm parameters  $(A_c, B_c, C_c, D_c)$ . To avoid cancelation of the integrator's pole in the loop, we assume that  $\det(A_2 - I) \neq 0$  and  $D_2 + C_2(I - A_2)^{-1}B_2 \neq 0$ .

With standard tools, the configuration in Fig. 6 can be subsumed to that in Fig. 2. The zero entries in the direct feedthrough terms of (36) are resulting from the integrator. By following the recipe in Sec. VI, we can hence compute optimal rates and close-to-optimal algorithms for this optimization problem under communication constraints.

If choosing  $G_1(z) = G_2(z) = 1$ , Fig. 6 is identical to Fig. 2 for standard optimization. With  $z_0 = 0$  in our synthesis procedure, we recover both the optimal convergence rates and the algorithm parameters for gradient decent ( $l = 0$ ) and  $\rho_{tm} := 1 - \sqrt{\frac{m}{L}}$  for the triple moment algorithm ( $l = 1$ ) [1], [6], [7]. Remarkably, Theorem 8 permits to show that  $\rho_{tm}$  is indeed the best possible rate that is achievable among all algorithms and any  $l \in \mathbb{N}_0$  [13, Corollary 4.8].

In the subsequent numerical experiments, we pick  $z_0 = 10^{-4}$ ,  $l = 2$  and compute the optimal convergence rates for the choices of the communication filters in Fig. 7. The results are plotted over the condition number  $\frac{L}{m}$  of the class  $\mathcal{S}_{m,L}$ .

If compared to the triple momentum algorithm (Case 2), the rates increase if the gradients are processed with a one-step delay (Case 3), but they are still mostly better than gradient descent (Case 1). For larger values of  $\frac{L}{m}$ , this is even true for delays in both channels (Case 4). Our approach allows for unstable dynamics in the optimization loop (Case 5), which affects the convergence rates adversely.

Figs. 8 and 9 depict the iterates with the optimal algorithm in Case 4, both for the quadratic and non-quadratic functions  $f(x, y) = Lx^2 + my^2$  and  $f(x, y) = \frac{1}{2}(x^2 + y^2) + 9\log(\exp(-x) + \exp(x/3 + y) + \exp(x/3 - y))$  [27] with  $m = 1$  and  $L = 10$ , respectively. The optimal rates (depicted by the black line) are matched in the quadratic case and give an upper bound for the non-quadratic function. Gradient decent fails to converge in both cases.

Finally, Fig. 10 reveals that optimal algorithms are work-



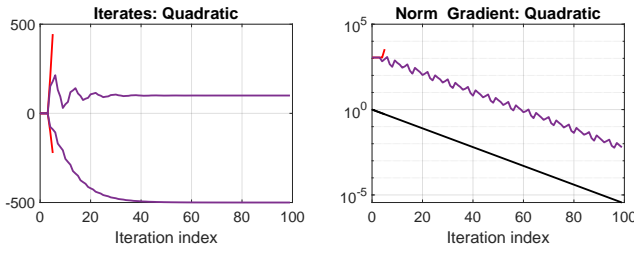


Fig. 8. Iterates for Case 4 with  $\frac{L}{m} = 10$  and a quadratic function for optimal algorithm (purple) and gradient decent (red). The black line indicates the optimal rate for synthesis.

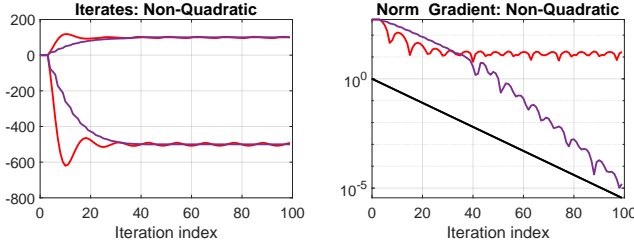


Fig. 9. Plots corresponding to Fig. 8 for a non-quadratic function.

ing well for the classes of functions they are designed for. As expected from robust control, however, they can be sensitive to deviations from the assumptions, as they lead to instability for the class  $\mathcal{S}_{1,11}$  that is only slightly larger than  $\mathcal{S}_{1,10}$ .

## VIII. CONCLUSIONS

In this paper we have presented the full pipeline to design optimal optimization algorithms or extremum controllers based on causal dynamic stability multipliers. A novel parametrization of these filters overcomes technical assumptions as required in previous work. Future work should be devote to the incorporation of anti-causal multipliers and performance objectives in synthesis.

## REFERENCES

[1] Y. Nesterov, *Lectures on Convex Optimization*, ser. Springer Optimization and Its Applications. Springer International Publishing, 2018, vol. 137.  
[2] B. Polyak, *Introduction to Optimization*. Optimization Software, Inc., New York, 1987.

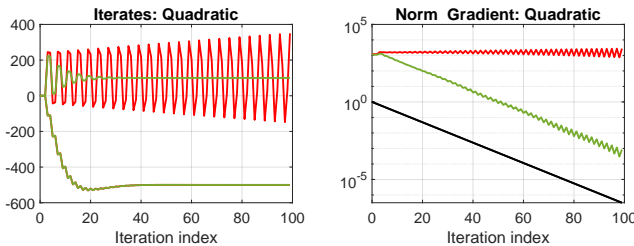


Fig. 10. Iterates for Case 5 with optimal algorithm designed for  $\frac{L}{m} = 10$ , implemented for a quadratic function with  $\frac{L}{m} = 10$  (green) and  $\frac{L}{m} = 11$  (red), respectively. The black line indicates the optimal rate for synthesis.

[3] J. Wang and N. Elia, "A control perspective for centralized and distributed convex optimization," in *Proceedings of the IEEE Conference on Decision and Control and European Control Conference, Orlando, FL, 2011*.  
[4] H.-B. Dürr and C. Ebenbauer, "On a class of smooth optimization algorithms with applications in control," *IFAC Proc.* vol. 45, no. 17. Elsevier BV, 2012, pp. 291–298.  
[5] L. Lessard, B. Recht, and A. Packard, "Analysis and Design of Optimization Algorithms via Integral Quadratic Constraints," *SIAM Journal on Optimization*, vol. 26, no. 1, pp. 57–95, 2016.  
[6] Y. Nesterov, "A method for unconstrained convex minimization problem with the rate of convergence  $O(\frac{1}{k^2})$ ," *Doklady AN SSSR*, vol. 269, pp. 543–547, 1983, (In Russian; translated as SovietMath. Docl.).  
[7] B. V. Scoy, R. A. Freeman, and K. M. Lynch, "The fastest known globally convergent first-order method for minimizing strongly convex functions," *IEEE Control Systems Letters*, vol. 2, no. 1, pp. 49–54, 2018.  
[8] L. Lessard and P. Seiler, "Direct synthesis of iterative algorithms with bounds on achievable worst-case convergence rate," in *2020 American Control Conference*, 2020, pp. 119–125.  
[9] S. Michalowsky, C. Scherer, and C. Ebenbauer, "Robust and structure exploiting optimisation algorithms: an integral quadratic constraint approach," *International Journal of Control*, vol. 94, pp. 1–24, 2021.  
[10] D. Gramlich, C. Ebenbauer, and C. W. Scherer, "Synthesis of accelerated gradient algorithms for optimization and saddle point problems using Lyapunov functions and LMIs," *Systems & Control Letters*, vol. 165, 2022.  
[11] A. B. Taylor, J. M. Hendrickx, and F. Glineur, "Smooth strongly convex interpolation and exact worst-case performance of first-order methods," *Mathematical Programming*, vol. 161, no. 1-2, pp. 307–345, 2016.  
[12] A. B. Taylor and Y. Drori, "An optimal gradient method for smooth strongly convex minimization," *Mathematical Programming*, vol. 199, no. 1-2, pp. 557–594, 2022.  
[13] C. Scherer and C. Ebenbauer, "Convex synthesis of accelerated gradient algorithms," *SIAM Journal on Control and Optimization*, vol. 59, no. 6, pp. 4615–4645, 2021.  
[14] T. Holicki and C. W. Scherer, "Algorithm design and extremum control: Convex synthesis due to plant multiplier commutation," in *60th IEEE Conference on Decision and Control*, 2021, pp. 3249–3252.  
[15] C. W. Scherer, "Robust exponential stability and invariance guarantees with general dynamic O'Shea-Zames-Falb multipliers," in *Proc. IFAC World Congress*, to appear, 2023.  
[16] A. Beck, *First-Order Methods in Optimization*. Society for Industrial and Applied Mathematics, 2017.  
[17] C. Desoer and M. Vidyasagar, *Feedback Systems: Input-Output Approach*. London: Academic Press, 1975.  
[18] A. Megretski and A. Rantzer, "System analysis via Integral Quadratic Constraints," *IEEE T. Automat. Contr.*, vol. 42, pp. 819–830, 1997.  
[19] J. Willems and R. Brockett, "Some new rearrangement inequalities having application in stability analysis," *IEEE T. Automat. Contr.*, vol. 13, no. 5, pp. 539–549, 1968.  
[20] G. Zames and P. L. Falb, "Stability conditions for systems with monotone and slope-restricted nonlinearities," *SIAM Journal of Control*, vol. 6, pp. 89–109, 1968.  
[21] R. Boczar, L. Lessard, and B. Recht, "Exponential convergence bounds using integral quadratic constraints," in *54th IEEE Conference on Decision and Control (CDC)*, 2015, pp. 7516–7521.  
[22] B. Hu and P. Seiler, "Exponential decay rate conditions for uncertain linear systems using integral quadratic constraints," *IEEE Transactions on Automatic Control*, vol. 61, no. 11, pp. 3631–3637, 2016.  
[23] C. W. Scherer, "Dissipativity and integral quadratic constraints: Tailored computational robustness tests for complex interconnections," *IEEE Control Systems Magazine*, vol. 42, no. 3, pp. 115–139, 2022.  
[24] P. Gahinet and P. Apkarian, "A linear matrix inequality approach to  $H_\infty$  control," *Internat. J. Robust Nonlinear Control*, vol. 4, pp. 421–448, 1994.  
[25] T. Iwasaki and R. Skelton, "All controllers for the general  $\mathcal{H}_\infty$  control problem: LMI existence conditions and state space formulas," *Automatica*, vol. 30, pp. 1307–1317, 1994.  
[26] P. Gahinet, "A new parametrization of  $H_\infty$  suboptimal controllers," pp. 1031–1051, 1994.  
[27] L. Lessard, "The analysis of optimization algorithms: A dissipativity approach," *IEEE Control Systems Magazine*, vol. 42, no. 3, pp. 58–72, 2022.



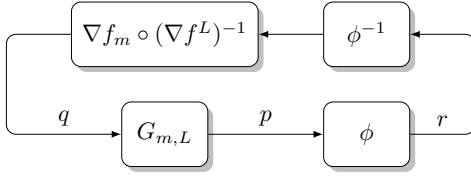


Fig. 11. Classical loop with stability multiplier.

- [28] K. J. Aström and R. M. Murray, *Feedback Systems: An Introduction for Scientists and Engineers*. Princeton University Press, 2009.  
 [29] E. de Souza and S. Bhattacharyya, "Controllability, observability and the solution of  $AX - XB = C$ ," *Linear Algebra and its Applications*, vol. 39, pp. 167–188, 1981.

## IX. RELATIONS TO CLASSICAL PASSIVITY THEORY

To explain the relation of Theorems 3 and 7 to the classical passivity theorem, we consider the case  $\rho = 1$  and assume that  $f^L$  is strongly convex. Then  $\nabla f^L : \mathbb{R}^d \rightarrow \mathbb{R}^d$  has a global inverse  $(\nabla f^L)^{-1} : \mathbb{R}^d \rightarrow \mathbb{R}^d$ . Let us abbreviate the system (24) with (23) and the filter (34) as

$$p = G_{m,L}(q) \quad \text{and} \quad r = \phi(p).$$

If filtering the signals of the loop (5)-(6) as in (22), a simple calculation leads to the interconnection

$$q = \nabla f_m \circ (\nabla f^L)^{-1}(p) \quad \text{and} \quad p = G_{m,L}(q) \quad (49)$$

as depicted in Fig. 11 in case that  $\phi$  is the static gain 1. Since the state-trajectories of the respective linear systems are identical, stability of the original loop (5)-(6) is equivalent to that of the transformed loop (49).

Next note that (20)-(22) translate into the fact that the new map  $\nabla f_m \circ (\nabla f^L)^{-1}$  is passive. Moreover, (25) just expresses that  $-G_{m,L}$  is strictly passive. Therefore, the passivity theorem guarantees that the new loop (49) is asymptotically stable. Hence, Theorem 3 boils down to this classical result applied to new loop (49). Note that the transformation of  $\nabla f$  into  $\nabla f_m \circ (\nabla f^L)^{-1}$  can be interpreted as taking nonlinearities that are slope restricted to the sector  $[m, L]$  into passive maps. Moreover, strict passivity of  $-G_{m,L}$  translates, by the KYP-Lemma, into the classical circle criterion expressed in terms of the transfer function of the linear system (6).

Even more, by Lemma 6,  $\phi$  and  $\phi^{-1}$  are both stable. Hence, guaranteeing stability of the loop (5)-(6) is equivalent to guaranteeing stability of the loop in Fig. 11 involving some nontrivial multiplier  $\phi$  in a classical sense. Lemma 5 then just means that  $q = \nabla f_m \circ (\nabla f^L)^{-1}(\phi^{-1}r)$  is passive for any multiplier  $\phi$  subject to (32). Moreover, Theorem 7 based on (35) expresses that  $-\phi G_{m,L}$  is strictly passive for some multiplier  $\phi$  subject to (32). Hence, Theorem 7 is an incarnation of the passivity theorem with causal multipliers as addressed in detail in [17, Chapter 9], with the additional feature of merging the reduction of conservatism over the passivity theorem with a corresponding computational search over a convex family of multipliers.

All this illustrates the key ideas underlying the more powerful general dissipativity theory involving integral quadratic constraints [23].

## X. APPENDIX: PROOFS AND AN AUXILIARY RESULT

### A. Proof of Lemma 2

The proof starts with standard arguments in convex analysis. Set  $\alpha := L - m > 0$ . Fix any  $y \in \mathbb{R}^d$  and define

$$g(x) := f_m(x) - \nabla f_m(y)^\top x \quad \text{for } x \in \mathbb{R}^n.$$

Clearly,  $g$  is convex since it is an affine perturbation of the convex function  $f_m$ . Due to  $\alpha q(x) - g(x) = Lq(x) - f(x) + \nabla f_m(y)^\top x$ , we conclude that  $\alpha q - g$  is also convex. An application of the subgradient inequality for  $\alpha q - g$  leads to

$$g(x+h) \leq g(x) + \nabla g(x)^\top h + \alpha q(h) \quad (50)$$

for all  $x, h \in \mathbb{R}^d$ . Since  $\nabla g(y) = \nabla f_m(y) - \nabla f_m(y) = 0$ , we conclude  $g(y) \leq g(x+h)$  and hence, with (50), that

$$g(y) \leq g(x) + \nabla g(x)^\top h + \alpha q(h) \quad \text{for all } x, h \in \mathbb{R}^d.$$

The minimum of the convex quadratic function in  $h$  on the right is easily calculated as  $g(x) - \frac{1}{\alpha} q(\nabla g(x))$ . This implies

$$\alpha g(y) \leq \alpha g(x) - q(\nabla g(x)) \quad \text{for all } x \in \mathbb{R}^d.$$

Simple rearrangements lead to (2). Indeed, with the definition of  $g$  and  $q(u-v) = q(u) + v^\top(v-u) - q(v)$  for  $u = \nabla f_m(x)$ ,  $v = \nabla f_m(y)$ , we get

$$\alpha f_m(y) - \alpha f_m(x) - \alpha v^\top(y-x) \leq -q(u) - v^\top(v-u) + q(v)$$

and this gives

$$[\alpha f_m(y) - q(v)] - [\alpha f_m(x) - q(u)] \leq v^\top[\alpha y - v - (\alpha x - u)].$$

Since  $\alpha y - v = (L - m)y - \nabla f(y) + my = Ly - \nabla f(y)$  and  $\alpha x - u = Lx - \nabla f(x)$ , we finally get

$$\begin{aligned} & [\alpha f_m(y) - q(\nabla f_m(y))] - [\alpha f_m(x) - q(\nabla f_m(x))] \leq \\ & \leq \nabla f_m(y)^\top [Ly - \nabla f(y) - (Lx - \nabla f(x))]. \end{aligned}$$

This is (2). In case of  $f \in \mathcal{S}_{m,L}^0$  we infer  $V(0) = 0$  by its very definition. Since  $\nabla f_m(0) = 0$ , we can apply (2) for  $u = 0$  to infer that  $V$  is indeed globally nonnegative.

### B. Proof of Theorem 3

Due to (25) and using standard rules for the Kronecker product, there exist some  $\varepsilon > 0$  with

$$\begin{aligned} & \bullet^\top \begin{pmatrix} \mathcal{X} \otimes I_d & 0 \\ 0 & -(\mathcal{X} \otimes I_d) \end{pmatrix} \begin{pmatrix} \mathcal{A} \otimes I_d & \mathcal{B} \otimes I_d \\ I & 0 \end{pmatrix} + \\ & + \bullet^\top \begin{pmatrix} 0 & I_d \\ I_d & 0 \end{pmatrix} \begin{pmatrix} \mathcal{C} \otimes I_d & \mathcal{D} \otimes I_d \\ 0 & I_d \end{pmatrix} + \begin{pmatrix} \varepsilon I & 0 \\ 0 & 0 \end{pmatrix} \preccurlyeq 0. \end{aligned} \quad (51)$$

Now pick any trajectory of (5)-(6). This can be transformed into one of (16)-(17) and filtered by (22) to generate a trajectory of (24). Right-multiplying (51) with  $\text{col}(\bar{x}_t, \bar{q}_t)$  and left-multiplying the transposed signal then leads to the dissipation inequality

$$\bar{x}_{t+1}^\top (\mathcal{X} \otimes I_d) \bar{x}_{t+1} - \bar{x}_t^\top (\mathcal{X} \otimes I_d) \bar{x}_t + 2\bar{q}_t^\top \bar{p}_t + \varepsilon \|\bar{x}_t\|^2 \leq 0$$

for all  $t \in \mathbb{N}_0$ . Now we exploit that the loop trajectories are as well related as in (17). From (22) and (21) we infer  $\bar{p}_t = \bar{F}^L(t, \bar{z}_t)$ ,  $\bar{q}_t = \bar{F}_m(t, \bar{z}_t)$ , which shows  $\sum_{t=0}^{T-1} \bar{q}_t^\top \bar{p}_t \geq$

0 for all  $T \in \mathbb{N}$  due to (20). Summation of the dissipation inequality for  $t = 0, \dots, T-1$  hence implies

$$\bar{x}_T^\top (\mathcal{X} \otimes I_d) \bar{x}_T - \bar{x}_0^\top (\mathcal{X} \otimes I_d) \bar{x}_0 + \varepsilon \sum_{t=0}^{T-1} \|\bar{x}_t\|^2 \leq 0 \quad (52)$$

for all  $T \in \mathbb{N}$ . If  $0 < k_- < k_+$  denote the smallest and largest eigenvalues of  $\mathcal{X} \otimes I_d$ , we conclude

$$k_- \|\bar{x}_T\|^2 + \varepsilon \sum_{t=0}^{T-1} \|\bar{x}_t\|^2 \leq k_+ \|\bar{x}_0\|^2 \quad \text{for all } T \in \mathbb{N}. \quad (53)$$

Since  $\bar{x}_T = \rho^{-T} x_T$  and  $\bar{x}_0 = x_0$ , we obtain (26) with  $K = k_+/k_-$ . For  $\rho = 1$ , we can conclude from (53) that  $\varepsilon \sum_{t=0}^{\infty} \|x_t\|^2 < \infty$  and, hence,  $\lim_{t \rightarrow \infty} x_t = 0$ .

### C. Proof of Lemma 4

Fix  $\nu \in \mathbb{N}$  and define  $z_t := \rho^t \bar{z}_t$  for  $t \in \mathbb{N}_0$ . From (2) and (19) we infer for all  $t \in \mathbb{N}_0$  that

$$\begin{aligned} V(z_t) - V(z_{t-\nu}) &\leq \nabla f_m(z_t)^\top [\nabla f^L(z_t) - \nabla f^L(z_{t-\nu})], \\ V(z_t) &\leq \nabla f_m(z_t)^\top \nabla f^L(z_t). \end{aligned}$$

The conic combination with the coefficients  $\rho^{-2(t-\nu)} \geq 0$  and  $\rho^{-2t} - \rho^{-2(t-\nu)} = \rho^{-2t}(1 - \rho^{2\nu}) \geq 0$  gives

$$\begin{aligned} \rho^{-2t} V(z_t) - \rho^{-2(t-\nu)} V(z_{t-\nu}) &\leq \\ &\leq \nabla f_m(z_t)^\top [\rho^{-2t} \nabla f^L(z_t) - \rho^{-2(t-\nu)} \nabla f^L(z_{t-\nu})]. \end{aligned} \quad (54)$$

The right hand side equals

$$\begin{aligned} \rho^{-t} \nabla f_m(z_t)^\top [\rho^{-t} \nabla f^L(z_t) - \rho^{-t} \rho^{-(t-\nu)} \nabla f^L(z_{t-\nu})] &= \\ = \bar{F}_m(t, \bar{z}_t)^\top (\bar{F}^L(t, \bar{z}_t) - \rho^\nu \bar{F}^L(t-\nu, \bar{z}_{t-\nu})). \end{aligned} \quad (55)$$

Now note for the left-hand side of (54) that

$$\begin{aligned} \sum_{t=0}^{T-1} (\rho^{-2t} V(z_t) - \rho^{-2(t-\nu)} V(z_{t-\nu})) &= \\ = \sum_{t=0}^{T-1} \rho^{-2t} V(z_t) - \sum_{t=-\nu}^{T-1-\nu} \rho^{-2t} V(z_t) &= \sum_{t=T-\nu}^{T-1} \rho^{-2t} V(z_t) \geq 0, \end{aligned}$$

where we exploited  $V(z_t) = 0$  for  $t < 0$ . Summation of (54) and using (55) hence proves (27).

### D. Proof of Lemma 5

Let  $\mu_\nu := -\lambda_\nu \rho^{-\nu} \geq 0$  for  $\nu \in \mathbb{N}$  and  $\mu_0 := \sum_{\nu=1}^{\infty} \mu_\nu$ . Then  $\lambda_0 - \mu_0 = \lambda_0 + \sum_{\nu=1}^{\infty} \lambda_\nu \rho^{-\nu} > 0$ . Let us now conically combine (20) and (27) to infer for any  $T \in \mathbb{N}$  that

$$0 \leq (\lambda_0 - \mu_0) \sum_{t=0}^{T-1} \bar{q}_t^\top \bar{p}_t + \sum_{\nu=1}^{\infty} \mu_\nu \sum_{t=0}^{T-1} \bar{q}_t^\top [\bar{p}_t - \rho^\nu \bar{p}_{t-\nu}].$$

Since  $\mu_0 := \sum_{\nu=1}^{\infty} \mu_\nu$ , this simplifies to

$$0 \leq \lambda_0 \sum_{t=0}^{T-1} \bar{q}_t^\top \bar{p}_t + \sum_{t=0}^{T-1} \bar{q}_t^\top \left[ \sum_{\nu=1}^t (-\mu_\nu \rho^\nu) \bar{p}_{t-\nu} \right],$$

where we also exploited that  $\bar{p}_{t-\nu} = \bar{F}^L(t-\nu, \bar{z}_{t-\nu}) = 0$  for  $\nu > t$ . Recalling the definition of  $\mu_\nu$  leads to

$$0 \leq \sum_{t=0}^{T-1} \bar{q}_t^\top \left[ \lambda_0 \bar{p}_t + \sum_{\nu=1}^t \lambda_\nu \bar{p}_{t-\nu} \right] = \sum_{t=0}^{T-1} \bar{q}_t^\top \bar{r}_t$$

which was to be shown.

### E. Proof of Lemma 6

We start by proving the equivalence of the first properties in (28) and (32) (for (31)). Indeed, (28) implies  $\lambda_\nu \leq 0$  for  $\nu = 0, \dots, l-1$ , which gives  $\mathbf{C}_f \mathcal{K}(A_f, B_f) \leq 0$ . Conversely,  $\mathbf{C}_f \mathcal{K}(A_f, B_f) \leq 0$  implies  $\mathbf{C}_f A_f^\nu B_f \leq 0$  for  $\nu = 0, \dots, l-1$ . By the Cayley-Hamilton theorem, we note that

$$\mathbf{C}_f A_f^{l+\mu} B_f = \sum_{j=0}^{l-1} (-\alpha_j) \mathbf{C}_f A_f^{j+\mu} B_f \quad \text{for all } \mu \in \mathbb{N}_0. \quad (56)$$

Since  $\alpha_j \leq 0$  for  $j = 0, \dots, l-1$ , we conclude from (56) for  $\mu = 0$  that  $\mathbf{C}_f A_f^l B_f \leq 0$ . An induction step based on (56) for  $\mu \in \mathbb{N}$  then proves  $\mathbf{C}_f A_f^\nu B_f \leq 0$  for all  $\nu = l+1, l+2, \dots$ .

Since  $A_f$  has all its eigenvalues in  $\mathbb{D}_\rho$ , we note next that

$$\sum_{\nu=0}^{\infty} (\mathbf{C}_f A_f^\nu B_f) z^{-(\nu+1)} = \mathbf{C}_f (zI - A_f)^{-1} B_f \quad \text{if } |z| \geq \rho. \quad (57)$$

Using (57) for  $z = \rho$  shows that the second conditions in (28) and (32) (for (31)) are as well equivalent.

Finally, assume that (32) holds. Based on (57) for  $z = \rho > 0$ , we can as well infer  $\mathbf{C}_f (\rho I - A_f)^{-1} B_f \leq 0$  and thus  $\mathbf{D}_f > 0$ . Then let  $\lambda \in \mathbb{C}$  be an eigenvalue of  $A_f - B_f \mathbf{D}_f^{-1} \mathbf{C}_f$  with  $|\lambda| \geq \rho$ . Since  $\alpha(\lambda) \neq 0$ , we infer that  $\mathbf{D}_f + \mathbf{C}_f (\lambda I - A_f)^{-1} B_f = 0$ . Again with (57), we infer

$$\begin{aligned} 0 &= |\mathbf{D}_f + \mathbf{C}_f (\lambda I - A_f)^{-1} B_f| \geq \\ &\geq \mathbf{D}_f - \sum_{\nu=1}^{\infty} |\mathbf{C}_f A_f^\nu B_f| |\lambda|^{-\nu} \geq \mathbf{D}_f - \sum_{\nu=1}^{\infty} |\mathbf{C}_f A_f^\nu B_f| \rho^{-\nu} = \\ &= \mathbf{D}_f + \sum_{\nu=1}^{\infty} (\mathbf{C}_f A_f^\nu B_f) \rho^{-\nu} = \mathbf{D}_f + \mathbf{C}_f (\rho I - A_f)^{-1} B_f > 0. \end{aligned}$$

This contradiction concludes the proof.

### F. Proof of Theorem 7

We follow the proof of Theorem 3. This leads to a trajectory of (24), but now for the matrices (35) and with the state-trajectory  $\text{col}(\xi_t, \bar{x}_t)$  comprising both the one of the filter (34) and the system (16). Since  $\xi_0 = 0$ , we conclude as earlier that

$$\begin{pmatrix} \xi_t \\ \bar{x}_t \end{pmatrix}^\top \underbrace{\begin{pmatrix} \mathcal{X}_f & \mathcal{X}_{fs} \\ \mathcal{X}_{sf} & \mathcal{X}_s \end{pmatrix}}_{\mathcal{X} \otimes I_d} \begin{pmatrix} \xi_t \\ \bar{x}_t \end{pmatrix} + \varepsilon \left\| \begin{pmatrix} \xi_t \\ \bar{x}_t \end{pmatrix} \right\|^2 \leq \bar{x}_0^\top \mathcal{X}_s \bar{x}_0$$

holds for all  $t \in \mathbb{N}_0$ , where  $\mathcal{X} \otimes I_d$  is partitioned according to  $\mathcal{A} \otimes I_d$  in (35). It remains to observe that the left-hand side can be bounded from below by  $\bar{x}_t^\top (\mathcal{X}_s - \mathcal{X}_{sf} \mathcal{X}_f^{-1} \mathcal{X}_{fs}) \bar{x}_t + \varepsilon \|\bar{x}_t\|^2$  and that the appearing Schur-complement is positive definite. This permits to conclude the proof as earlier.

### G. Proof of Theorem 8

Proof of (a)  $\Rightarrow$  (b). By a slight perturbation of  $(\mathbf{C}_f, \mathbf{D}_f)$ , we can make sure that

$$(\mathbf{A}_f, \mathbf{C}_f) \text{ is observable and no eigenvalue of } \tilde{A} \text{ is a zero of } \beta(z) := [\mathbf{D}_f + \mathbf{C}_f (zI - \mathbf{A}_f)^{-1} B_f] \alpha(z) \quad (58)$$

and (25), (32) still hold. Then all assumptions in Lemma 9 are satisfied for (44). Note that  $\beta(z) = \mathbf{D}_f \alpha(z) +$

$C_f \text{col}(1, z, \dots, z^{l-1})$ . Hence, equations 1)-4) in Lemma 9 match with those formulated in the theorem, and (45) is invertible. By (32) and Lemma 6, we conclude that

$$A_f^i := A_f - B_f D_f^{-1} C_f \text{ is Schur.} \quad (59)$$

Moreover, (70) in Lemma 9 implies

$$\left( \begin{array}{c|c|c} T \hat{A} T^{-1} & T \hat{B}_1 & T \hat{B} \\ \hline \hat{C}_z T^{-1} & \hat{D}_{zw} & \hat{D}_z \end{array} \right) = \left( \begin{array}{c|c|c} A_f & 0 & T_f \hat{B}_1 \\ \hline \tilde{B} C_f & \tilde{A} & \tilde{T} \hat{B}_1 \\ \hline \tilde{D}_z C_f & \tilde{C}_z & \tilde{D}_{zw} \end{array} \right). \quad (60)$$

In the sequel, we exploit the obvious relation

$$\left( \begin{array}{c} A_f \\ \tilde{B} C_f \\ \tilde{D}_z C_f \end{array} \right) = \left( \begin{array}{c} A_f^i \\ 0 \\ 0 \end{array} \right) + \left( \begin{array}{c} B_f \\ \tilde{B} D_f \\ \tilde{D}_z D_f \end{array} \right) D_f^{-1} C_f. \quad (61)$$

Our first goal is to construct some annihilators  $\hat{U}$  and  $\hat{V}$  with (40). By inspection,  $\hat{U}$  as given in the theorem already has this property. For convexification, some specific  $\hat{V}$  needs to be constructed on the basis of  $V$  in (46). To this end, we note that (46) and  $D_f \neq 0$  imply

$$\ker((T \hat{B})^\top \hat{E}^\top) = \ker(B_f^\top D_f \tilde{B}^\top D_f \tilde{D}_z^\top) \supset \text{im} \left( \begin{array}{c} 0 \\ V_2^\top \\ V_3^\top \end{array} \right)$$

if partitioning the columns of  $V$  as  $(V_2 \ V_3)$  accordingly. Thus, we can determine  $V_f, \hat{V}_2, \hat{V}_3$  such that

$$\left( \begin{array}{c|c} V_f^\top & 0 \\ \hline \hat{V}_2^\top & V_2^\top \\ \hline \hat{V}_3^\top & V_3^\top \end{array} \right) \text{ is a basis of } \ker(\hat{B}^\top T^\top \hat{E}^\top). \quad (62)$$

As a consequence, (40) is satisfied with the choice

$$\hat{V} := \left( \begin{array}{c|c|c} V_f & \hat{V}_2 & \hat{V}_3 \\ \hline 0 & V_2 & V_3 \end{array} \right) \left( \begin{array}{c} T \ 0 \\ \hline 0 \ I \end{array} \right). \quad (63)$$

By construction, we note that  $V_f$  has full row rank.

By our preparatory remarks, it is then guaranteed that there exist symmetric matrices  $X$  and  $\hat{Y}$  with (41)-(43).

Let us now introduce

$$Y := T \hat{Y} T^\top = \left( \begin{array}{c|c} Y_f & \bullet \\ \hline \bullet & \hat{Y} \end{array} \right). \quad (64)$$

A congruence transformation of (43) then leads to

$$\left( \begin{array}{c|c} Y & T \\ \hline T^\top & X \end{array} \right) = \left( \begin{array}{c|c|c} Y_f & \bullet & T_f \\ \hline \bullet & \hat{Y} & \tilde{T} \\ \hline T_f^\top & \tilde{T}^\top & X \end{array} \right) \succ 0. \quad (65)$$

Canceling the first block row and column shows (48).

In moving towards (47), we note that (42) is equivalent to

$$\underbrace{\hat{V} \left( \begin{array}{c|c|c} -T^{-1} & \hat{A} T^{-1} & 0 \\ \hline 0 & \hat{C}_z T^{-1} & -1 \end{array} \right)}_F \left( \begin{array}{c|c|c} Y & 0 & 0 \\ \hline 0 & -Y & 0 \\ \hline 0 & 0 & 1 \end{array} \right) \bullet^\top \succ 0. \quad (66)$$

Due to (63), the product of the two matrices on the left equals

$$F = \left( \begin{array}{c|c|c} V_f & \hat{V}_2 & \hat{V}_3 \\ \hline 0 & V_2 & V_3 \end{array} \right) \left( \begin{array}{c|c|c} -I & T \hat{A} T^{-1} & 0 \\ \hline 0 & \hat{C}_z T^{-1} & -1 \end{array} \right) \begin{array}{c} T \hat{B} \\ \hat{D}_{zw} \end{array}.$$

If we recall (60) and exploit (61) with (62), this reads as

$$F = \left( \begin{array}{c|c|c} V_f & \hat{V}_2 & \hat{V}_3 \\ \hline 0 & V_2 & V_3 \end{array} \right) \left( \begin{array}{c|c|c|c} -I & 0 & A_f^i & 0 \\ \hline 0 & -I & 0 & \tilde{A} \\ \hline 0 & 0 & 0 & \tilde{C}_z \end{array} \right) \begin{array}{c} 0 \\ T_f \hat{B}_1 \\ \tilde{T} \hat{B}_1 \\ -1 \end{array} \begin{array}{c} \hat{D}_{zw} \end{array}. \quad (67)$$

Canceling the first block row gives

$$(V_2 \ V_3) \left( \begin{array}{c|c|c} 0 & -I & 0 \\ \hline 0 & 0 & \tilde{C}_z \end{array} \right) \begin{array}{c} \tilde{A} \\ 0 \\ -1 \end{array} \begin{array}{c} \tilde{T} \hat{B}_1 \\ \hat{D}_{zw} \end{array}.$$

As a consequence, after canceling the first block row and column of (66) and if recalling (64), we arrive at (47).

Proof of (b)  $\Rightarrow$  (a). Suppose that (32), (41) and (47)-(48) are feasible. By perturbing  $(C_f, D_f)$  if necessary, we can again assume that (58) holds true. Due to (59), we can solve the Stein equation  $Y_f - A_f^i Y_f (A_f^i)^\top = I$  and note that  $Y_f \succ 0$ . Motivated by (64), we define

$$\hat{Y} = T^{-1} \left( \begin{array}{c|c} \gamma Y_f & 0 \\ \hline 0 & \hat{Y} \end{array} \right) T^{-\top} \quad (68)$$

with some still to-be-determined scalar  $\gamma > 0$ . For this choice of  $\hat{Y}$  and in view of (67), the inequalities (65)-(66) read as

$$\left( \begin{array}{c|c} \gamma Y_f & S_{12} \\ \hline S_{21} & S_{22} \end{array} \right) \succ 0 \text{ and } \left( \begin{array}{c|c} \gamma V_f V_f^\top + R_{11} & R_{12} \\ \hline R_{21} & R_{22} \end{array} \right) \succ 0, \quad (69)$$

respectively, where the  $R$ - and  $S$ -blocks are independent from  $\gamma$ . Moreover, (48) and (47) just guarantee that  $S_{22} \succ 0$  and  $R_{22} \succ 0$ . Since  $Y_f \succ 0$  and  $V_f V_f^\top \succ 0$  (because  $V_f$  has full row rank), we can choose  $\gamma$  sufficiently large in order to enforce the validity of (69), and thus of (65)-(66) with  $Y = \text{diag}(\gamma Y_f, \hat{Y})$ . Again, these translate back into (42)-(43). In summary, we have shown the existence of  $X$  and  $\hat{Y}$  to guarantee (41)-(43), which in turn implies the existence of a controller as was to be shown.

## H. On Commuting Transfer Functions

*Lemma 9:* For SISO transfer functions with realizations

$$G = \left[ \begin{array}{c|c} A & B \\ \hline C & D \end{array} \right] \text{ and } \hat{G} = \left[ \begin{array}{c|c} \hat{A} & \hat{B} \\ \hline \hat{C} & \hat{D} \end{array} \right],$$

let  $\alpha$  and  $\hat{\alpha}$  denote the characteristic polynomials of  $A \in \mathbb{R}^{n \times n}$ ,  $\hat{A} \in \mathbb{R}^{\hat{n} \times \hat{n}}$ , respectively, and define the polynomial  $\beta := G\alpha$  of degree at most  $n$ .

Let  $(A, B)$  and  $(A, C)$  be controllable and observable, respectively, and suppose that  $(A, \hat{A})$  have no common eigenvalues and  $(\beta, \hat{\alpha})$  and  $(\alpha, \hat{G})$  no common zeros in  $\mathbb{C}$ .

Then the two standard realizations of the products in  $G\hat{G} = \hat{G}G$  are related by a state-coordinate change as

$$\left[ \begin{array}{c|c|c} A & B\hat{C} & B\hat{D} \\ \hline 0 & \hat{A} & \hat{B} \\ \hline C & D\hat{C} & D\hat{D} \end{array} \right] \xrightarrow{\left( \begin{array}{c|c} L^{-1} & -L^{-1}K \\ \hline NL^{-1} & M - NL^{-1}K \end{array} \right)} \left[ \begin{array}{c|c|c} A & 0 & B \\ \hline \hat{B}C & \hat{A} & \hat{B}D \\ \hline \hat{D}C & \hat{C} & \hat{D}D \end{array} \right] \quad (70)$$

with the solutions of the matrix equations

- 1)  $AK - K\hat{A} + B\hat{C} = 0$ ,
- 2)  $LK(A, B) = K(A, B\hat{D} - K\hat{B})$ ,
- 3)  $M\alpha(\hat{A}) = \beta(\hat{A})$ ,
- 4)  $\hat{A}N - NA + \hat{B}C = 0$ .

**Proof. Preparation.** Note that  $G = D + \gamma\alpha^{-1}$  for  $\gamma := \beta - D\alpha$ . With the coefficients of  $\alpha(z) = \alpha_0 + \dots + \alpha_{n-1}z^{n-1} + z^n$  and  $\gamma(z) = \gamma_0 + \gamma_1z + \dots + \gamma_{n-1}z^{n-1}$ , and next to the companion matrix  $C_\alpha$  of  $\alpha$ , let us define

$$H_\alpha := \begin{pmatrix} \alpha_1 & \dots & \alpha_{n-1} & 1 \\ \vdots & & \vdots & \vdots \\ \alpha_{n-1} & \dots & 0 & 0 \\ 1 & \dots & 0 & 0 \end{pmatrix}, \quad B_\gamma := \begin{pmatrix} \gamma_0 \\ \vdots \\ \gamma_{n-2} \\ \gamma_{n-1} \end{pmatrix}.$$

With the polynomial vectors  $r_n(z) = (z^0 \ z^1 \ \dots \ z^{n-1})$  and  $c_n(z) = r_n(z)^T$ , the Kalman controllability and observability matrices of  $(A, B)$ ,  $(A, C)$  can be directly expressed as  $r_n(A)(I_n \otimes B)$ ,  $(I_n \otimes C)c_n(A)$ , respectively. Then  $S := r_n(A)(I_n \otimes B)H_\alpha$  is invertible and guarantees [28]

$$S^{-1}AS = C_\alpha, \quad S^{-1}B = e_n \quad \text{and} \quad CS = B_\gamma^T. \quad (71)$$

Analogously,  $T := H_\alpha(I_n \otimes C)c_n(A)$  is invertible with

$$TAT^{-1} = C_\alpha^T, \quad TB = B_\gamma \quad \text{and} \quad CT^{-1} = e_n^T. \quad (72)$$

*Step 1.* Since  $A$  and  $\hat{A}$  have no common eigenvalues, the solutions  $K$  and  $N$  of the Sylvester equations 1) and 4) exist and are unique. With these two equations we get

$$\left( \begin{array}{c|c|c} A & B\hat{C} & B\hat{D} \\ \hline 0 & \hat{A} & \hat{B} \\ \hline C & D\hat{C} & D\hat{D} \end{array} \right) \xrightarrow{\begin{pmatrix} I & -K \\ 0 & I \end{pmatrix}} \left( \begin{array}{c|c|c} A & 0 & B\hat{D} - K\hat{B} \\ \hline 0 & \hat{A} & \hat{B} \\ \hline C & D\hat{C} + CK & D\hat{D} \end{array} \right), \quad (73)$$

$$\left( \begin{array}{c|c|c} A & 0 & B \\ \hline 0 & \hat{A} & B\hat{D} - NB \\ \hline \hat{D}C + \hat{C}N & \hat{C} & \hat{D}D \end{array} \right) \xrightarrow{\begin{pmatrix} I & 0 \\ 0 & N \end{pmatrix}} \left( \begin{array}{c|c|c} A & 0 & B \\ \hline \hat{B}C & \hat{A} & \hat{B}D \\ \hline \hat{D}C & \hat{C} & \hat{D}D \end{array} \right). \quad (74)$$

Since  $G\hat{G} = \hat{G}G$ , the transfer functions defined by both sides of (73) and (74) are identical and decompose as in

$$\left[ \begin{array}{c|c} A & B\hat{D} - K\hat{B} \\ \hline C & D\hat{D} \end{array} \right] + \left[ \begin{array}{c|c} \hat{A} & \hat{B} \\ \hline D\hat{C} + CK & D\hat{D} \end{array} \right] = \left[ \begin{array}{c|c} A & B \\ \hline \hat{D}C + \hat{C}N & \hat{D}D \end{array} \right] + \left[ \begin{array}{c|c} \hat{A} & B\hat{D} - NB \\ \hline \hat{C} & \hat{D}D \end{array} \right]. \quad (75)$$

*Step 2.* The goal is to prove that  $L^{-1}$  is invertible and

$$\left( \begin{array}{c|c} A & B\hat{D} - K\hat{B} \\ \hline C & D\hat{D} \end{array} \right) \xrightarrow{L^{-1}} \left( \begin{array}{c|c} A & B \\ \hline \hat{D}C + \hat{C}N & \hat{D}D \end{array} \right). \quad (76)$$

By (75) and since  $A$  and  $\hat{A}$  share no eigenvalues, the system's transfer functions on the left and on the right of (76) are indeed identical. Let us now prove respectively, that

$(A, B\hat{D} - K\hat{B}), (A, \hat{D}C + \hat{C}N)$  is controllable, observable.

Indeed, suppose that  $x^*A = \lambda x^*$  and  $x^*(B\hat{D} - K\hat{B}) = 0$ . Then 1) gives  $x^*K(\lambda I - \hat{A}) + x^*B\hat{C} = 0$  and thus  $x^*K = -x^*B\hat{C}(\lambda I - \hat{A})^{-1}$ . This implies  $0 = x^*(B\hat{D} - K\hat{B}) = x^*B(\hat{D} + \hat{C}(\lambda I - \hat{A})^{-1}\hat{B}) = x^*B\hat{G}(\lambda)$ . Since  $\alpha(\lambda) = 0$ ,

we infer  $\hat{G}(\lambda) \neq 0$  and thus  $x^*B = 0$ . This shows  $x^* = 0$ , just because  $(A, B)$  is controllable. Hence  $(A, B\hat{D} - K\hat{B})$  is controllable. The Sylvester equation 4) for  $N$  permits to similarly prove that  $(A, \hat{D}C + \hat{C}N)$  is observable.

As a conclusion, the realizations of the identical transfer functions in (76) are minimal. This guarantees the existence of  $L$  with (76), and  $L^{-1}$  satisfies  $L^{-1}K(A, B\hat{D} - K\hat{B}) = K(A, B)$  [28]. In summary, we have shown that 2) has a unique invertible solution  $L$  which guarantees (76).

*Step 3.* Since no eigenvalue of  $\hat{A}$  is a zero of  $\alpha$  and  $\beta$ , both  $\alpha(\hat{A})$  and  $\beta(\hat{A})$  are invertible. Therefore,  $M$  as in 3) exists and is unique and invertible.

Now we prove that

$$\left( \begin{array}{c|c} \hat{A} & \hat{B} \\ \hline D\hat{C} + CK & D\hat{D} \end{array} \right) \xrightarrow{M} \left( \begin{array}{c|c} \hat{A} & \hat{B}D - NB \\ \hline \hat{C} & \hat{D}D \end{array} \right). \quad (77)$$

By its very definition,  $M$  commutes with  $\hat{A}$ , which implies  $M\hat{A}M^{-1} = \hat{A}$ . To prove  $\hat{C}M = D\hat{C} + CK$ , we observe (see e.g. [29, Proof of Lemma 4]) that 1) implies

$$\alpha(A)K - K\alpha(\hat{A}) + r_n(A)(I_n \otimes B)H_\alpha(I_n \otimes \hat{C})c_n(\hat{A}) = 0.$$

If using  $\alpha(A) = 0$ , we infer with  $S$  from (71) that

$$K = S(I_n \otimes \hat{C})c_n(\hat{A})\alpha(\hat{A})^{-1}. \quad (78)$$

Since  $\hat{C}$  and  $C$  are rows, we have  $CS(I_n \otimes \hat{C}) = (CS \otimes 1)(I_n \otimes \hat{C}) = (CS \otimes \hat{C}) = (1 \otimes \hat{C})(CS \otimes I_n) = \hat{C}(CS \otimes I_n)$ . By using (71), we hence conclude from (78) that

$$CK = \hat{C}(B_\gamma^T \otimes I_n)c_n(\hat{A})\alpha(\hat{A})^{-1} = \hat{C}\gamma(\hat{A})\alpha(\hat{A})^{-1}.$$

Finally, recall  $\beta = D\alpha + \gamma$  and thus  $\beta(\hat{A}) = D\alpha(\hat{A}) + \gamma(\hat{A})$ . By 3), this leads to  $M = DI_n + \gamma(\hat{A})\alpha(\hat{A})^{-1}$  and then  $\hat{C}M = \hat{C}D + \hat{C}\gamma(\hat{A})\alpha(\hat{A})^{-1} = D\hat{C} + CK$ , as to be shown.

In complete analogy, 4) implies with  $T$  from (72) that

$$N = -\alpha(\hat{A})^{-1}r_n(\hat{A})(I_n \otimes \hat{B})T.$$

This leads to

$$NB = -\alpha(\hat{A})^{-1}r_n(\hat{A})(B_\gamma \otimes I_n)\hat{B} = -\alpha(\hat{A})^{-1}\gamma(\hat{A})\hat{B}.$$

Then  $M\hat{B} = D\hat{B} + \alpha(\hat{A})^{-1}\gamma(\hat{A})\hat{B} = \hat{B}D - NB$ .

*Step 4.* Continuing (73) with (77) and (76) leads to

$$\left( \begin{array}{c|c|c} A & B\hat{C} & B\hat{D} \\ \hline 0 & \hat{A} & \hat{B} \\ \hline C & D\hat{C} & D\hat{D} \end{array} \right) \xrightarrow{\begin{pmatrix} I & K \\ 0 & M \end{pmatrix}} \left( \begin{array}{c|c|c} A & 0 & B\hat{D} - K\hat{B} \\ \hline 0 & \hat{A} & \hat{B}D - NB \\ \hline C & \hat{C} & D\hat{D} \end{array} \right) \xrightarrow{\begin{pmatrix} L^{-1} & -L^{-1}K \\ 0 & M \end{pmatrix}} \left( \begin{array}{c|c|c} A & 0 & B \\ \hline 0 & \hat{A} & \hat{B}D - NB \\ \hline \hat{D}C + \hat{C}N & \hat{C} & \hat{D}D \end{array} \right).$$

In combination with (74), the matrix

$$\begin{pmatrix} I & 0 \\ N & I \end{pmatrix} \begin{pmatrix} L^{-1} & -L^{-1}K \\ 0 & M \end{pmatrix} = \begin{pmatrix} L^{-1} & -L^{-1}K \\ NL^{-1} & M - NL^{-1}K \end{pmatrix}$$

indeed guarantees (70). This latter definition also shows that the transformation matrix is invertible. ■